5-2007

Effects of pH on Human Cardiac and Neuronal Sodium Channels

William James Israelsen
Utah State University

EFFECTS OF pH ON HUMAN CARDIAC AND NEURONAL SODIUM CHANNELS

by

William James Israelsen

Thesis submitted in partial fulfillment of the requirements for the degree

of

DEPARTMENTAL HONORS

in

Biology
in the Department of Biology

Approved:

Thesis/Project Advisor (Dr. Peter C. Ruben)	**Departmental Honors Advisor** (Dr. Kimberly A. Sullivan)

Director of Honors Program
(Dr. Christie L. Fox)

UTAH STATE UNIVERSITY
Logan, UT

Spring 2007

Effects of pH on human cardiac and neuronal sodium channels

Honors Thesis

William J. Israelsen
Department of Biology, Utah State University, Logan, Utah, 84322

Introduction

Voltage-gated sodium channels are large transmembrane proteins that selectively allow the passage of sodium ions across the cell membrane in response to membrane depolarizations (Yu and Catterall, 2003). The resulting influx of positive charge further depolarizes the membrane and is responsible for the upstroke of the action potential. Voltage-gated sodium channels are vital to the initiation and propagation of action potentials in excitable cells such as neurons and myocytes. In vertebrates, there are many different tissue-specific sodium channel isoforms; these include the neuronal ($Na_V1.2$) and cardiac ($Na_V1.5$) isoforms. Although very closely related in structure and functional characteristics, the different channel types have unique functional properties well suited to the physiological functions of their respective tissues.

Under certain pathological conditions *in vivo*, including ischemia caused by heart attack or stroke, sodium channels are exposed to an acidic environment. The increase in acidity resulting from ischemia is harmful to the affected tissue and often leads to cell death. The pH changes during heart attack and stroke are often rather dramatic. Normal physiological pH is 7.4, but during global cerebral ischemia for example, the extracellular pH typically falls by approximately 1 pH unit to around 6.4 and the intracellular pH also falls to an average pH of 6.4 as well (Lipton, 1999). Similarly, global ischemia in rat hearts results in a reduction of the average intracellular pH down to 6.2 (Garlick et al., 1979).

Changes in pH have been shown to affect sodium channel function. At low pH, sodium channels exhibit proton block due to the large increase in proton concentration. Proton block of the channel results in reduced sodium conductance; this is observed in recordings of macroscopic sodium current (Benitah et al., 1997; Khan et al., 2002) and in single channel recordings (Zhang and Siegelbaum, 1991; Benitah et al., 1997). Most studies to date have considered the mechanism of proton block without investigating the role that low pH may play in modulating fast inactivation and slow inactivation. Fast and slow inactivation are both important functional states of the sodium channel. In general, the purpose of this research is to more fully determine how the functional characteristics of neuronal and cardiac sodium channels are affected by increased proton concentrations. A more specific purpose of this research is to determine whether there is a connection between proton block and channel gating.

Proton block, channel gating, and the other functional properties of sodium channels are determined by channel structure. Sodium channels are multimeric proteins; they consist of a large, pore-forming α-subunit and smaller β1 and β2 subunits (Marban et al., 1998; Vilin and Ruben, 2001). The α-subunit is made up of four homologous domains (labeled DI-DIV), which are arranged in ring-like fashion around a central pore. Each of these four domains is comprised of six transmembrane segments (labeled S1-S6). The S4 segments, one from each domain, contain positively-charged amino acids and act as the primary voltage sensors of the channel. The channel pore itself is formed by the S5-S6 linkers, or p-loops. Additionally, three amino acid residues on the DIII-DIV linker (isoleucine, phenylalanine, methionone: IFM) form what is known as the fast inactivation particle on the intracellular side of the protein.

The structure of a voltage-gated sodium channel contributes to its function (Marban et al., 1998). For example, movement of the S4 segments in response to a membrane depolarization activates the channel, allowing the flow of sodium ions through the pore. Within milliseconds of activation, the fast inactivation particle binds to its docking site on the underside of the channel and occludes the pore. The channel is now fast inactivated and influx of sodium ions stops. Slow inactivation occurs on the order of tens of seconds in response to repeated or prolonged membrane depolarizations. It is thought that slow inactivation is due to an occlusion or collapse of the pore brought about by further movement of the S4 segments (Vilin and Ruben, 2001).

Recent models of proton block and the channel pore have implicated a ring of four carboxylate amino acids (glutamate, glutamate, aspartate, aspartate: EEDD), one on each p-loop in the pore, as the probable site for titration of protons which could result in proton block of the channel (Khan et al., 2002). The p-loops are also a main structural determinant of slow inactivation in sodium channels (Vilin et al., 1999), and a recent study demonstrated that charge neutralizations or reversals of the negatively-charged EEDD residues in the pore enhance entry into the slow inactivated state and retard recovery from that state (Xiong et al., 2006). Additionally, fast inactivation is affected by charge reversal or neutralization of two negatively-charged glutamate residues adjacent to the IFM particle (McCollum et al., 2003). These changes in charge decrease the probability of slow inactivation and stabilize fast inactivation.

Both fast and slow inactivation could therefore be affected by charge neutralization of any critical carboxylate residues through titration with hydrogen ions at low pH. Protonation of the aspartate or glutamate residues in the channel pore might speed slow inactivation onset and retard slow inactivation recovery, and protonation of the glutamate residues near the fast inactivation particle could stabilize fast inactivation and decrease the probability of slow inactivation. It is important to note, however, that there are many more structural determinants of fast and slow inactivation, making the above predictions, which are based on only a small part of the whole picture, very tentative. Further complications arise in that there is a reciprocal relationship between fast and slow inactivation (Richmond et al., 1998), and the local environment of the glutamate residues flanking the fast inactivation particle may not be conducive to their protonation at any physiologically relevant pH.

Using mammalian expression systems, the aim of this set of experiments is to determine the effects of low pH on $Na_V1.2$ and $Na_V1.5$ channels. $Na_V1.2$ is of special interest due to the lack of previous work and because of its role as the arch-typical brain sodium channel. A comparison of the effects of different pH environments and the structural differences between the two isoforms may shed light on the structure/function relationship of the channels and provide useful information about the effects of ischemia *in vivo*. The experiments simulate the pH levels experienced by the sodium channels during normal physiological conditions, ischemia, and then reperfusion and the resulting return to normal pH.

Materials and Methods

Cell Preparation: HEK293 cells (American Type Culture Collection) were made to express human $Na_V1.5$ by transient transfection with a mixture of two separate plasmids, one containing channel cDNA and the other containing the gene for Enhanced Green Fluorescent Protein, which was used to locate successfully transfected cells during recording. The transfections were done using Polyfect transfection agent (Qiagen) when the cells were approximately 50% confluent. After an overnight incubation, the cells were re-suspended and

plated onto small recording squares cut from glass microscope slide cover slips. Recordings were made the following day.

A line of stably-transfected CHO cells expressing $Na_V1.2$ (a kind gift from the Catterall lab) was grown in DMEM/F12 medium containing the antibiotic G418 as a selective agent. The cells were plated onto recording squares and incubated overnight in preparation for recording the following day.

Electrophysiology: Whole cell patch clamp recordings were made from both types of cells at pH 7.4 and pH 6.0. The pH 7.4 extracellular recording solutions contained (in mM): 140 NaCl, 4 KCl, $2CaCl_2$, 1 $MgCl_2$, 5 glucose, 10 HEPES. The pH was adjusted using 1N CsOH. The pH 6.0 extracellular solution contained (in mM): 130 NaCl, 4 KCl, $2CaCl_2$, 1 $MgCl_2$, 5 glucose, 10 MES. The pH was adjusted using 1N HCL. The reduction in sodium chloride concentration of the pH 6.0 solution was to compensate for the additional 10 mM Na^+ provided by the MES buffer, which is a sodium salt. The sodium concentration of both extracellular solutions was therefore 140 mM, and the pH of both solutions was adjusted at 22° C. The intracellular solutions contained (in mM): 130 CsCl, 10 NaCl, 10 EGTA, 10 HEPES, 4 Mg-ATP, and 0.38 Li-GTP, for HEK293 recording; or 105 CsF, 40 Cs, 10 NaCl, 10 Cs-EGTA, and 10 HEPES, for CHO recording. Importantly, both intracellular solutions contained 10 mM Na^+.

Micropipette electrodes were made from borosilicate glass pulled with a Sutter pipette puller. The ends of the electrodes were coated with dental wax to reduce capacitance and the tips were fire-polished before use. The micropipette electrodes had a resistance of 2-3 megaohms.

Electrophysiological recordings were made using an EPC-9 patch-clamp amplifier (HEKA, Lambrecht, Germany) and Pulse/Pulsefit software (HEKA) run on a Macintosh computer. The pulse protocols were conducted control-experiment-control at pHs of 7.4, 6.0, and 7.4 as follows: The recording chamber was filled with pH 7.4 extracellular solution and the bath temperature was equilibrated to 22° C using a Peltier device controlled by a temperature controller. A recording plate was placed in the recording chamber, and the cells were perfused with 2 ml of recording solution to remove any traces of growth medium. A seal was established between the microelectrode and the membrane of a lone, spherical cell. Cells were only used if the seal showed a resistance greater than 1 gigaohm. After a 30 second stabilization time, suction was used to break the cell membrane within the pipette tip to gain access to interior of the cell. The membrane potential was then held at –100 mV and the cell was checked for sodium current after another short wait. The HEK cells were then ready for immediate recording, but CHO cells required an additional 5 minute stabilization period before data was collected.

All experimental pulse protocols were first run in the pH 7.4 control solution (control). Using a perfusion system, the bath solution was then replaced with pH 6.0 recording solution (experiment), and the experimental protocols were run again after a two minute wait. Finally, the low pH recording solution was replaced with the pH 7.4 control solution (wash), 2 minutes were waited, and the recordings were repeated. Pulse protocols were used to record current amplitude, conductance as a function of voltage, and steady state fast and slow inactivation, as previously described (Richmond et al., 1998).

Data Analysis: Analysis and graphing were done using Pulsefit (HEKA) and Igor Pro (Wavemetrics, Lake Oswego, OR) software programs. Statistical analysis was done using InStat software. The I(V) curves were converted to conductance curves using the equation $g = I_{max} / (V_m - E_{rev})$ where g is conductance, I_{max} is the peak test pulse sodium current, V_m is the test pulse

voltage, and E_{rev} is the sodium reversal potential. The g(V) curves were fit using a Boltzmann function: $(g/g_{max}) = 1 / (1 + \exp(-ze_o(V_m - V_{1/2})/kT)$, where the term (g/g_{max}) is normalized sodium conductance, z is the apparent valence, e_o is the elementary charge, $V_{1/2}$ is the midpoint voltage, V_m is the test pulse voltage, k is the Boltzmann constant, and T is the temperature in Kelvin. Steady-state fast and slow inactivation data were normalized and fitted with Boltzmann functions. The equation $(I/I_{max}) = 1 / (1 + \exp(-ze_o(V_m - V_{1/2})/kT)$ was used for steady-state fast inactivation, where the term (I/I_{max}) is normalized current; and the equation $(I/I_{max}) = (1 - X) / (1 + \exp(-ze_o(V_m - V_{1/2})/kT) + X$ was used for slow inactivation, where the additional term X allows the final level of inactivation to be less than 100%.

The data from the experimental and wash pHs were compared to control using analysis of variance. The values of interest were the midpoint voltages (V_m), apparent valence (z), and maximum probability of slow inactivation of the curves, which is $(1 - X)$. Differences resulting in p-values less than 0.05, as determined from Student's t-test, were considered statistically significant.

Results

Proton Block: Both channel isoforms exhibit fully reversible proton block (Fig. 1). At pH 6.0, current amplitude is reduced by approximately 50% in both channel types, while a return to neutral pH results in sodium currents of amplitudes equal to those of the control.

Figure 1. Example of proton block at pH 6.0 in $Na_V1.5$

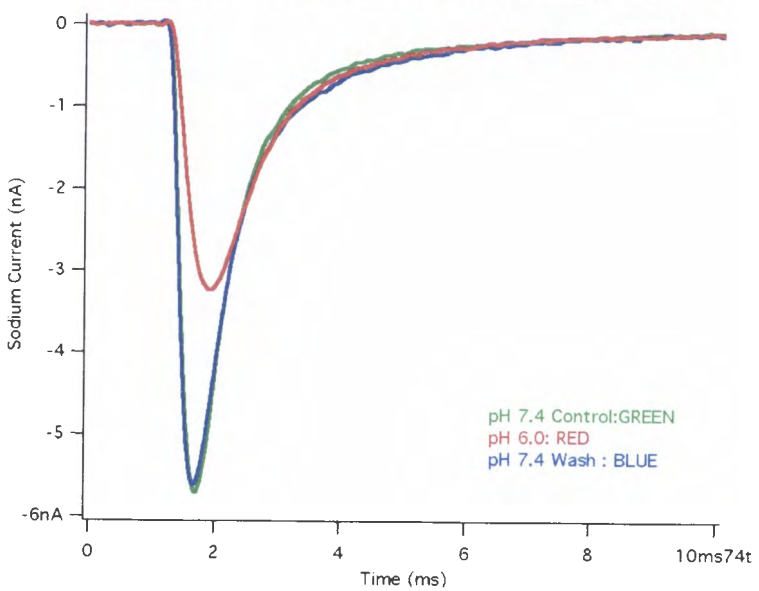

Conductance: Change in pH affects the conductance of both channel types, but the changes in conductance in the neuronal isoform are much larger than those in the cardiac isoform. Interestingly, only significant effect seen upon lowering the pH to 6.0 is a change in the slope of the neuronal conductance curve (Fig. 2). The drop in pH reduces the slope from 4.36 to 3.24 ($p=0.0220$). The return to neutral pH, however, caused a ~ -17 mV shift of the conductance midpoint ($p=0.0132$) in the neuronal sodium channel, and the same return to neutral pH resulted in a smaller, ~ -5 mV shift in the cardiac channel ($p=0.0377$).

Figure 2. g(V) of $Na_V1.2$

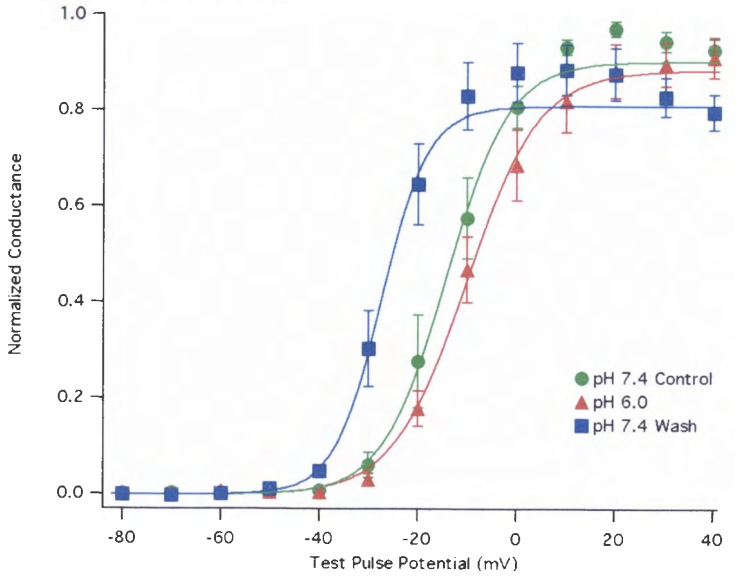

Figure 3. g(V) of $Na_V1.5$

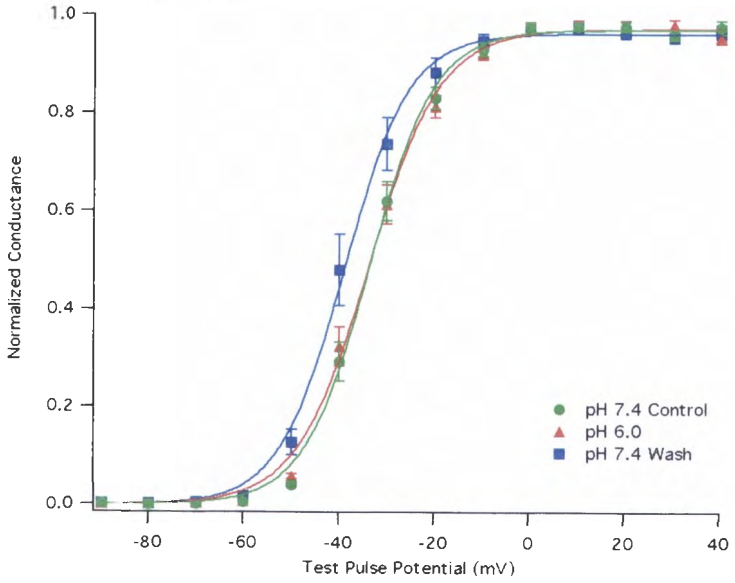

Steady-State Fast Inactivation: Both channels exhibit pH-induced effects on steady-state fast inactivation. The slopes and midpoints of the fast inactivation curves of both channels at pH 6.0 were not significantly different from those in the control condition. The only effects of pH were seen upon return to pH 7.4 from the acidic condition. The steady-state fast inactivation midpoints of both channel types were shifted in the hyperpolarizing direction upon return to neutral pH (Fig. 3 and 4). The midpoint of the neuronal channel curve was shifted ~ -11 mV ($p=0.0052$), and the midpoint of the cardiac channel curve was shifted ~ -6 mV ($p=0.002$). Return to pH 7.4 had no effect on the slope of the curve in the neuronal sodium channel, but in the cardiac channel, the slope of the pH 7.4 wash was significantly reduced to -3.36 from the control slope of -4.10 ($p=0.0104$).

Figure 4. Steady-State Fast Inactivation of $Na_V1.2$

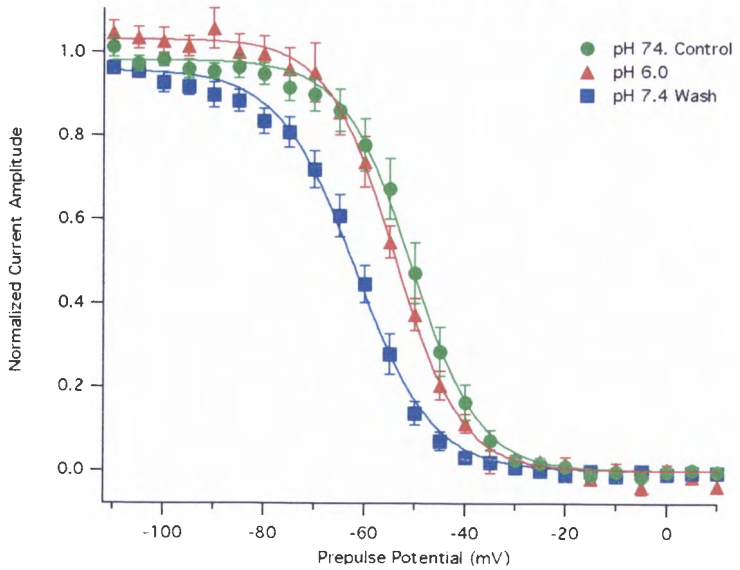

Figure 5. Steady-State Fast Inactivation of $Na_V1.5$

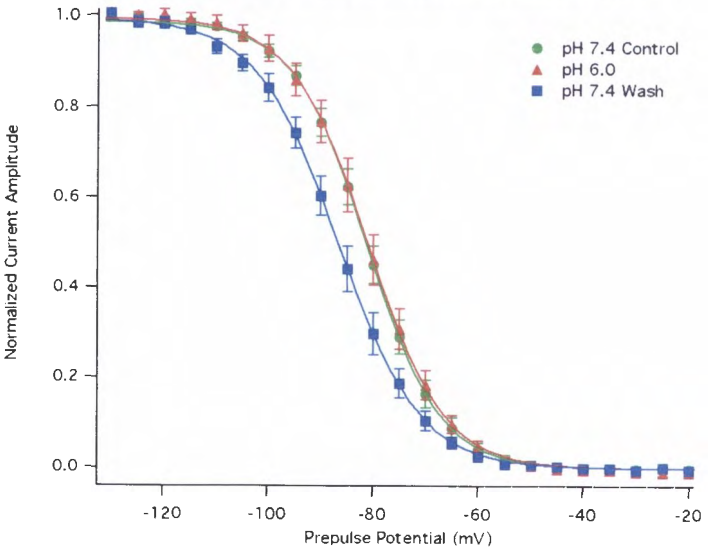

Steady-State Slow Inactivation: The levels of completion of the steady-state slow inactivation were not significantly affected by pH change in either isoform, but the levels of completion differed greatly between the neuronal and brain channels. Slow inactivation was ~85% complete in the brain channel (Fig. 6) and much less complete in the cardiac channel, only ~60% (data not shown). This is consistent with previous findings (Richmond et al., 1998; Vilin et al., 2001). The slope of the steady-state slow inactivation curve for the neuronal channel was not significantly affected by pH change. The midpoint of the $Na_V1.2$ curve was shifted ~ -5 mV when the pH was changed to 6.0 ($p=0.0564$). Return to pH 7.4 shifted the midpoint ~ -13 mV from the control ($p=0.0007$).

Figure 6. Steady-State Slow Inactivation of $Na_V1.2$

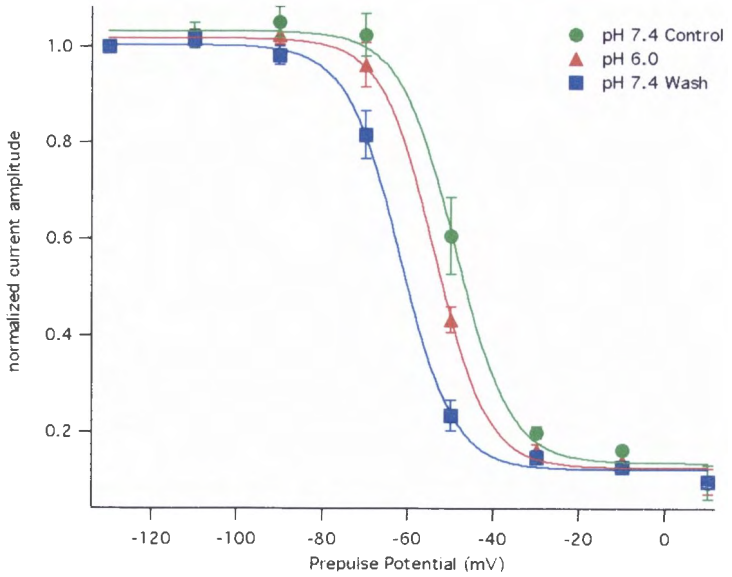

Discussion

With the exception of proton block itself, which was seen in both channel isoforms, the only significant effect observed in either channel due to increased acidity was a flattening of the slope of the neuronal conductance curve. The proton block observed in these experiments is consistent with previous results (Benitah et al., 1997; Khan et al., 2002). The change in slope indicates that the neuronal sodium channel becomes less voltage sensitive during conditions of high extracellular proton concentration. This effect was not observed at low pH in the cardiac isoform, but this is not surprising in light of the vital importance that properly controlled excitability of the heart plays in the survival of an individual during both normal and pathological conditions. It also suggests that there may be specific structural differences between the two isoforms which are responsible for the difference in the voltage sensitivity of activation. Notably, there are histidine residues located in the turret region proximal to the pore. These residues have been demonstrated to impart pH sensitivity to voltage-gated potassium channels and to affect the voltage sensitivity of channel gating (Fedida et al., 2005; Kwan et al., 2006). Significantly, $Na_V1.2$ has three histidine residues in the homologous turret region whereas Nav1.5 has only two histidines in the turret. This structural difference may account for the observed difference in pH sensitivity of channel gating in the present study.

Additionally, this study confirmed the previous observation that the cardiac sodium channel has a much lower maximum probability of slow inactivation relative to neuronal sodium channels (Richmond et al., 1998; Vilin et al., 2001). The low maximum probability of slow inactivation found in the cardiac isoform serves to ensure continued heart excitability and function after repeated depolarizations over long periods of time.

Interestingly, the greatest effects of pH on channel function were seen upon return to neutral pH from the acidic condition. Both channel types exhibited the same effects, but the changes in conductance and fast and slow inactivation in the neuronal channel were consistently greater than those in the cardiac channel. The hyperpolarizing shift in the voltage dependence of activation in both channels caused by return to neutral pH is consistent with an increase in

excitability. This increase in excitability may contribute to the excitotoxicity and reperfusion injury seen in the heart and brain following the restoration of blood flow after heart attack and stroke (Hou and MacManus, 2002; Takeo and Tanonaka, 2004). In contrast, the hyperpolarizing shift in the voltage dependence of both fast and slow inactivation indicates that fewer channels would be available for activation. More detailed studies would unravel the significance of these changes. At present, the primary conclusion that can be drawn from these data is that the hyperpolarizing effects on activation and inactivation of restoring normal pH further demonstrate the coupling between these biophysical processes.

Appendix

Table 1. Mean conductance and steady-state fast inactivation data

	g(V) Midpoint		g(V) Slope		SS FI Midpoint		SS FI Slope	
Channel Isoform	1.2	1.5	1.2	1.5	1.2	1.5	1.2	1.5
pH 7.4 Control	-12.85	-33.5	4.36	4.08	-51.15	-80.66	-3.98	-4.1
pH 6.0 Experiment	-7.94	-33.48	3.24*	4.25	-54.59	-81.17	-3.85	-3.73
pH 7.4 Wash	-24.98*	-38.52*	4.66	4.35	-61.88***	-86.60***	-3.47	-3.36**

* indicates $p<0.05$ vs. Control
** indicates $p<0.01$ vs. Control
*** indicates $p<0.001$ vs. Control

Table 2. Mean steady-state slow inactivation data

	SS SI Midpoint	SS SI Slope	SS SI Completion
Isoform	1.2	1.2	1.2
pH 7.4 Control	-49.25	-4.25	87%
pH 6.0 Experiment	-54.19	-5.24	81%
pH 7.4 Wash	-61.81***	-4.16	88%

* indicates $p<0.05$ vs. Control
** indicates $p<0.01$ vs. Control
*** indicates $p<0.001$ vs. Control

Works Cited

Benitah J, Balser JR, Marban E, Tomaselli GF (1997) Proton inhibition of sodium channels: mechanism of gating shifts and reduced conductance. J Membr Biol 155:121-131.

Fedida D, Zhang S, Kwan DC, Eduljee C, Kehl SJ (2005) Synergistic inhibition of the maximum conductance of Kv1.5 channels by extracellular K+ reduction and acidification. Cell Biochem Biophys 43:231-242.

Garlick PB, Radda GK, Seeley PJ (1979) Studies of acidosis in the ischaemic heart by phosphorus nuclear magnetic resonance. Biochem J 184:547-554.

Hou ST, MacManus JP (2002) Molecular mechanisms of cerebral ischemia-induced neuronal death. Int Rev Cytol 221:93-148.

Khan A, Romantseva L, Lam A, Lipkind G, Fozzard HA (2002) Role of outer ring carboxylates of the rat skeletal muscle sodium channel pore in proton block. J Physiol 543:71-84.

Kwan DC, Fedida D, Kehl SJ (2006) Single channel analysis reveals different modes of Kv1.5 gating behavior regulated by changes of external pH. Biophys J 90:1212-1222.

Lipton P (1999) Ischemic cell death in brain neurons. Physiol Rev 79:1431-1568.

Marban E, Yamagishi T, Tomaselli GF (1998) Structure and function of voltage-gated sodium channels. Journal of Physiology 508:647-657.

McCollum IJ, Vilin YY, Spackman E, Fujimoto E, Ruben PC (2003) Negatively charged residues adjacent to IFM motif in the DIII-DIV linker of hNa(V)1.4 differentially affect slow inactivation. FEBS Lett 552:163-169.

Richmond JE, Featherstone DE, Hartmann HA, Ruben PC (1998) Slow inactivation in human cardiac sodium channels. Biophysical Journal 74:2945-2952.

Takeo S, Tanonaka K (2004) Na+ overload-induced mitochondrial damage in the ischemic heart. Can J Physiol Pharmacol 82:1033-1043.

Vilin YY, Ruben PC (2001) Slow inactivation in voltage-gated sodium channels. Cell Biochemistry and Biophysics 35:171-190.

Vilin YY, Fujimoto E, Ruben PC (2001) A single residue differentiates between human cardiac and skeletal muscle Na+ channel slow inactivation. Biophysical Journal 80:2221-2230.

Vilin YY, Makita N, George AL, Ruben PC (1999) Structural determinants of slow inactivation in human cardiac and skeletal muscle sodium channels. Biophysical Journal 77:1384-1393.

Xiong W, Farukhi YZ, Tian Y, Disilvestre D, Li RA, Tomaselli GF (2006) A conserved ring of charge in mammalian Na+ channels: a molecular regulator of the outer pore conformation during slow inactivation. J Physiol 576:739-754.

Yu FH, Catterall WA (2003) Overview of the voltage-gated sodium channel family. Genome Biol 4:207.

Zhang JF, Siegelbaum SA (1991) Effects of external protons on single cardiac sodium channels from guinea pig ventricular myocytes. J Gen Physiol 98:1065-1083.